World Academy of Science, Engineering and Technology
International Journal of Aerospace and Mechanical Engineering
Vol:8, No:1, 2014

# A TIPSO-SVM Expert System for Efficient Classification of TSTO Surrogates

Ali Sarosh, Dong Yun-Feng, Muhammad Umer



***Abstract*—**Fully reusable spaceplanes do not exist as yet. This implies that design-qualification for optimized highly-integrated forebody-inlet configuration of booster-stage vehicle cannot be based on archival data of other spaceplanes. Therefore, this paper proposes a novel TIPSO-SVM expert system methodology. A non-trivial problem related to optimization and classification of hypersonic forebody-inlet configuration in conjunction with mass-model of the two-stage-to-orbit (TSTO) vehicle is solved. The hybrid-heuristic machine learning methodology is based on two-step improved particle swarm optimizer (TIPSO) algorithm and two-step support vector machine (SVM) data classification method. The efficacy of method is tested by first evolving an optimal configuration for hypersonic compression system using TIPSO algorithm; thereafter, classifying the results using two-step SVM method. In the first step extensive but non-classified mass-model training data for multiple optimized configurations is segregated and pre-classified for learning of SVM algorithm. In second step the TIPSO optimized mass-model data is classified using the SVM classification. Results showed remarkable improvement in configuration and mass-model along with sizing parameters.

***Keywords*—**TIPSO-SVM expert system, TIPSO algorithm, two-step SVM method, aerothermodynamics, mass-modeling, TSTO vehicle.

## I. Background

A classical vehicle design process relies heavily on archival design data for validation of its results. The classical methodology begins with initial size estimation – an iterative process that yields geometric parameters such as volume, wetted area, length etc. for vehicle and the stages. This is followed by vehicle weight estimation which is also an iterative process and parameters such as gross take-off/launch masses, empty masses etc. are obtained. Once mass and sizing model is complete then aerothermodynamic [1], [2] and aeroelastic studies [3] are undertaken to refine the configuration. Throughout these assessments the process relies greatly on archival (historical) design data of benchmark vehicles/systems. When optimization is undertaken for the final configuration its results are again compared with historical data, if desired improvement has been attained than approval is accorded to the conceptual design, else the process is repeated till desired optimal parameters have been achieved. The high level of dependence on archival data may be well justified in the wake of large amount of data available for benchmark launch vehicles, however the same is not possible for spaceplanes in either single- or two-stage i.e. SSTO/TSTO configurations. This is because no real hypersonic fully-reusable trans-atmospheric vehicle exists as yet. Under this scenario any methodology based on archival data may not suffice. Fig. 1 depicts the typical classical design methodology.

In view of the foregoing in this paper a hybrid heuristic-intelligent methodology is proposed as an expert system. The process mitigates the effect of dependence on historical data and instead uses computational intelligence [4] as its chief source for verification of results. It is used to solve the non-trivial problem of evolving a global solution that simultaneously satisfies optimization needs of highly-integrated hypersonic forebody-inlet configuration and mass-model of the corresponding TSTO vehicle. The proposed methodology optimizes the aerothermodynamic design of forebody-inlet assembly of the booster stage while simultaneously optimizing mass distribution for the TSTO vehicle. It uses a combination of TIPSO algorithm [5], [6] (for optimization) and a two-step SVM method [7] (for classification), in a hybrid arrangement, to recursively locate a global optimal solution for aerothermodynamic parameters of hypersonic compression component and attendant mass-model of the corresponding TSTO vehicle. The optimal solution is treated as a candidate configuration whose efficacy i.e. suitability is classified using support vector machine algorithm. This classification methodology acts as an expert system for mass-modeling parameters to evaluate suitability of the TSTO configuration. This method has the obvious advantage of substantially improving the efficiency of design process by obtaining a truly global optimal solution that satisfies the high-level integration need through synchronized optimization and classification of the component and corresponding vehicle respectively. The TIPSO-SVM expert system results when evaluated through vehicle sizing analysis show marked improvement in basic geometrical parameters of the vehicle.

Ali Sarosh is with the Department of Aerospace Engineering, National University of Sciences and Technology (NUST), Pakistan (phone: 0092-3349856088; e-mail: alisarosh@cae.nust.edu.cn, info@alisarosh.com).

Dong Yun-Feng is with the Department of Flight Vehicle Design, School of Astronautics, Beihang University (BUAA), 37 Xueyuan Road, Beijing 100191, P. R. China (e-mail:- sinosat@buaa.edu.cn).

Muhammad Umer is with the Department of Aerospace Engineering, National University of Sciences and Technology (NUST), Pakistan (phone: 0092-3333664906, e-mail: mhmdumer@gmail.com).

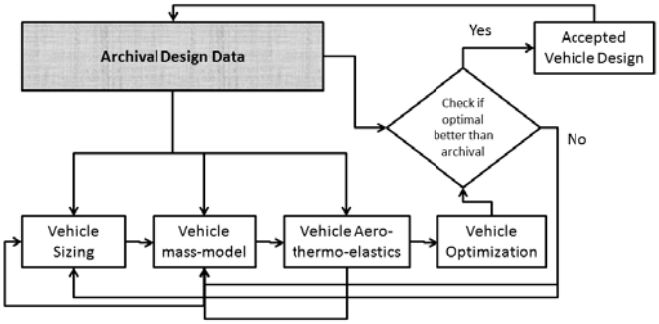


Fig. 1 Classical conceptual design approach

## II. The TIPSO-SVM Methodology

The TIPSO-SVM optimization and classification methodology is embedded within the design optimization framework of SHWAMIDOF-FI program [7]. This tri-modular program follows the configuration evolution, optimization and analysis process for forebody-inlet component and its TSTO vehicle as depicted in Fig. 2 below. This process has been evolved on the basis of cognitive-heuristic framework approach [8]. In brief the surrogates of forebody-inlet configurations are evolved using fast and frugal heuristic methods. A cognitive DF-APSO decision algorithm [9] is used to select the baseline configuration which is heuristically optimized using TIPSO algorithm [5]. The optimized solution yields aerothermodynamic-geometric design for compression component and a mass-model for the TSTO vehicle that constitutes the optimized compression components. Verification and validation of results are accomplished by analyzing the output parameters through SVM classification and high-fidelity CFD solutions. If acceptance is accorded to verification and validation parameters then TSTO vehicle sizing is accomplished for lower stage *booster* or else the cycle is repeated from optimization stage. The shaded blocks indicate process components that constitute the TIPSO-SVM methodology. This process has several peculiarities which are best understood by reviewing the optimization-classification process in detail.

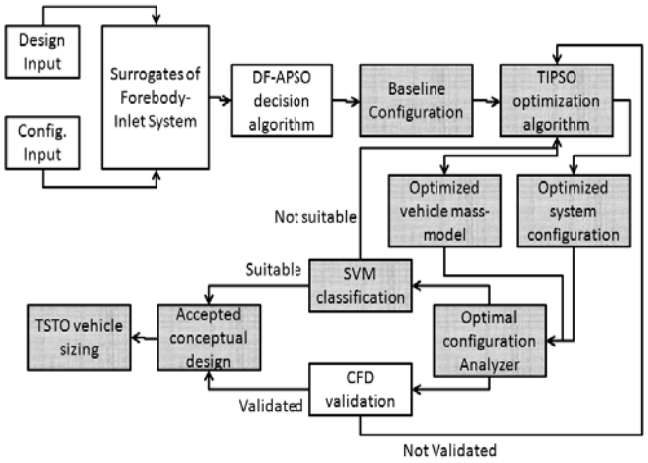


Fig. 2 Vehicle design process of SHWAMIDOF-FI program

The TIPSO-SVM hybridized method is depicted at Fig. 3 below. It uses aerothermodynamic data of hypersonic compression together with mass-model data for TSTO transatmospheric vehicle and optimizes the solution for maximization of process efficiencies and minimization of losses. A training data library of previously optimized mass-models is stored and when new data on optimization of vehicle mass-model is generated and passed to SVM it is classified for suitability by comparison with the stored training data. If the new data is classified as *suitable* it is stored and processed for vehicle sizing and an accepted conceptual design of vehicle is evolved. In case it fails the classification test then the data is returned back to optimization stage till an optimal solution can be achieved.

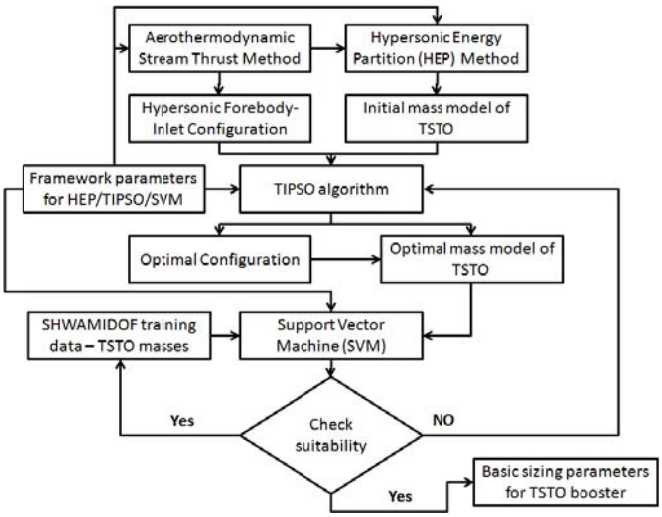


Fig. 3 General approach of the TIPSO-SVM expert system

## III. TIPSO Optimization Scheme

The TIPSO algorithm uses 17 solver functions to simultaneously optimize the aerothermodynamic design of hypersonic compression system and mass-model of the TSTO vehicle. Each of the unique solver function acts as objective functions (OF) and all OFs are related through a single aggregate objective function (AOF) which must be maximized for obtaining the MDO (multidisciplinary optimization) solution. Details of each of the OFs are presented solver wise as follows:-

### *A. Cone Solver Function*

$$f_1 = -\left(Cp/Cd\right) * \left(h_{\max}/dR\right) * \theta_S \qquad (1)$$

*Cp* and *Cd* are pressure and drag coefficients for semi-elliptical forebody, $h_{max}$ is the maximum height of generating cone, *dR* is the difference between the radii for generating and generated cones while $\theta s$ is the flow deflection angle of lower side of forebody.

*B. 1st Wedge (Ramp) Solver*

$$f_2 = -\left[\begin{matrix}\left(M_d/M_u\right)_1 + \left(p_d/p_u\right)_1 + \\ \left(\rho_d/\rho_u\right)_1 + \left(T_d/T_u\right)_1\end{matrix}\right]_{OSW1} * \beta_{1d} \quad (2)$$

Subscripts *d* and *u* represent downstream and upstream conditions across oblique shock wave generated from 1st wedge ramp. Symbols *M*, *p*, *ρ* and *T* represent Mach number, pressure, density and temperature conditions, while *β* represents shock wave angle of planar wedge. This description holds good for (3) and (4) as well.

*C. 2nd Wedge (Ramp) Solver*

$$f_3 = -\left[\begin{matrix}\left(M_d/M_u\right)_2 + \left(p_d/p_u\right)_2 + \\ \left(\rho_d/\rho_u\right)_2 + \left(T_d/T_u\right)_2\end{matrix}\right]_{OSW2} * \beta_{2d} \quad (3)$$

*D. Cowl Solver*

$$f_4 = -\left\{\begin{matrix}\left|\left(M_d - M_{d_{ref}}\right) + \left[\left(T_d/T_u\right) - \left(T_d/T_u\right)_{ref}\right] + \right. \\ \left.\left|\left[\left(p_d/p_u\right) - \left(p_d/p_u\right)_{ref}\right]\right|_{OSW3} \right. \\ * \beta_{3d}\end{matrix}\right\} \quad (4)$$

The *ref* parameters are suitably selected values of Mach number, temperature and pressure ratios that represent ideal conditions for flow entering the combustion chamber. These are framework values that are defined externally through a *.txt* file as input variables for the program.

*E. Compression System Solver*

$$f_5 = -\left(\eta_c + \eta_{KE} - \varsigma\right) \quad (5)$$

Variables $\eta_c$ and $\eta_{KE}$ represent compression and kinetic energy efficiencies while ς represents non-dimensional entropy losses for the hypersonic compression system, such that $\varsigma = ds/Cp_c$.

*F. Stream Thrust Solver*

$$f_6 = -\left(\eta_o * \eta_c\right) \quad (6)$$

The overall efficiency $\eta_o$ represents the overall thermodynamic performance of the HAP system.

*G. Inlet Start-Unstart Solver*

$$f_7 = -\left[\left(A_i/A_t\right)_{Kant} * \left(A_0/A_t\right)_{Emp} * \left(A_1/A_t\right)_{Isen}\right] * M_i \quad (7)$$

The symbols $A_i$, $A_0$, $A_1$ and $A_t$ represent inlet cross-section area, freestream capture area, inlet capture area and throat area of the inlet respectively while *Mi* refers to Mach number at inlet entry.

*H. Inlet-Isolator Interaction Solver*

$$f_8 = -\left[\left(p_3/p_2\right)_{\max} \Big/ \left(p_{3e}/p_{2i}\right)\right] * \mathrm{Re}_\theta \quad (8)$$

The numerator term $(p_3/p_2)_{max}$ in the square brackets represents the pressure ratio that could result in a normal shock wave, while the term $(p_{3e}/p_{2i})$ represents the instantaneous pressure ratio, both across the isolator. The term $Re_\theta$ is the Reynolds number of the momentum boundary layer.

*I. Inviscid Aerothermodynamics Solver*

$$f_9 = -\left[\begin{matrix}Cp_{WS} + Cp_{LS} + \\ Cl - Cd + Cr + \\ \left(L/D\right)_{comp} - \left(\Delta_1/\Delta_2\right)\end{matrix}\right] \Big/ \left(\left(R_N + R_L\right)/L_{body}\right) \quad (9)$$

The coefficient terms include pressure (*Cp*), lift (*Cl*), drag (*Cd*) and resultant force (*Cr*) while *L/D* ratio is essential to waverider configuration and $(\Delta_1/\Delta_2)$ are ratios of standoff distance at a given nose and lip radii ($R_N$ , $R_L$) respectively across body length ($L_{body}$).

*J. Leading Edge Bluntness & Shock Standoff Solver*

$$f_{10} = -\left[\left(p/p_0\right) \Big/ \left(\Delta_s/R_C\right)\right] * \left(L_{\max}/R_L\right) \quad (10)$$

The term $p/p_0$ is the instantaneous pressure ratio across normal shock region of shock wave, $\Delta_s$ represents the shock standoff distance (m), $R_c$ is the radius of curvature (m) of the shock wave while $L_{max}$ and $R_L$ represent maximum length (m) of the shock generation surface and radius (m) of the lip of the leading edge of cowl.

*K. Shock-Boundary Layer Interaction Solver*

$$f_{11} = -\left\{\begin{matrix}\left|\left(\delta_{invis} - \delta\right)/\delta\right| + \\ \left|\left[\left(T_d/T_u\right)_{invis} - \left(T_d/T_u\right)\right] \Big/ \left(T_d/T_u\right)\right| + \\ \left|\left[\left(p_d/p_u\right)_{invis} - \left(p_d/p_u\right)\right] \Big/ \left(p_d/p_u\right)\right|\end{matrix}\right\} \quad (11)$$

Equation (11) represents the measure of variations in flow deflection angle (*δ*) and flowfield variables temperature (*T*) and pressure (*p*) caused by shock-boundary layer interaction when compared with equivalent parameters obtained from inviscid (*invis*) solution.

*L. Stagnation Point Convective Heat Transfer Solver*

$$f_{12} = -\Omega = -\left[ \left( R_N * p_0 \right) \Big/ \left( \mu_0 * V_0 \right) \right] \tag{12}$$

Here $R_N$ represents nose radius in meters while subscript *0* represents freestream conditions. This relation is derived using Buckingham-Pi theorem.

*M. Thermal State of Surface Solver*

$$f_{13} = -\left\{ \Pr * \mathrm{Re}_X * St_X * \left[ Z_{tw} \left( 1 - Z_{t0} \right) \right] \right\} * C_f \tag{13}$$

The left hand term represents Prandtl number (*Pr*), local Reynolds number ($Re_x$) and local Stanton number ($St_x$). The terms $Z_{tw}$ and $Z_{to}$ are thermal state parameters for freestream and wall regions. They are derived using Buckingham-Pi theorem and expressed in (14) below.

$$\begin{aligned} Z_{t0} &= \left( T_0 * k_0 \right) \Big/ \left( \mu_0 * V_0^2 \right) \\ Z_{t0} &= \left( T_w * k_w \right) \Big/ \left( \mu_w * V_e^2 \right) \end{aligned} \tag{14}$$

*N. Boundary Layer Solver*

$$f_{14} = -\left[ L_{axial} \Big/ \left( \bar{\delta}_{flow} + \bar{\delta}_{disp} + \bar{\delta}_{mom} + \bar{C}_f - \bar{X}_{trans} \right) \right] \tag{15}$$

The $\delta$, $C_f$ and $X_{trans}$ bar symbols represent average parameter values for the flow along the lower side of the external compression surfaces.

*O. Hypersonic Viscous Interaction Solver*

$$f_{15} = -\left\{ \left[ \left( p_w / p_0 \right) \Big/ Cp \right] * Kn * \mathrm{Re}_X \right\} \tag{16}$$

where pressure ratio $p_w/p_0$ indicates increment in wall pressure conditions, *Cp* is the coefficient of pressure, *Kn* is the freestream Knudsen number and $Re_x$ is the local Reynolds number of flow in the viscous interaction region.

*P. Forebody-Inlet Geometry Integration Solver*

$$f_{16} = -\left( inlet\ ratio \Big/ volume\ ratio \right) * \left\{ \left[ \begin{matrix} \left( \beta_{0d} + \beta_{1d} + \beta_{2d} + \beta_{3d} \right) * \\ \left( p_{3e} / p_{2i} \right) \end{matrix} \right] \Big/ \left( h_{\max} * \mathrm{Re}_\theta \right) \right\} \tag{17}$$

where,

$$inlet\ ratio = w_{inlet} / h_{inlet}$$

$$Vol\ ratio = \left( L_{axial} * H_{\max} * W_{\max} \right) \Big/ A_{inlet} * L_{isolator}$$

The variables of right hand term in (17) are same as those described in (1) to (4) and (8). Variables $w_{inlet}$ and $h_{inlet}$ are the maximum width (m) and height (m) of inlet while $L_{axial}$ describes the total axial length of forebody-inlet assembly along the body coordinates, $H_{max}$ and $W_{max}$ are the maximum dimensions of the assembly measured along vertical and lateral directions respectively. The variable $A_{inlet}$ is area of inlet ($m^2$) determined geometrically from the aerothermodynamic solution while $L_{isolator}$ is length of isolator (m) obtained from solution of inlet-isolator interaction solver.

*Q. Mass Modeling Solver*

$$f_{17} = -\left\{ \begin{matrix} \left[ \left( Z * Z_e \right) / \Gamma_{TSTO} \right] + \\ \left[ \left( Z * Z_e \right) / \Gamma_{SSTO} \right] \end{matrix} \right\} * \left[ \left( L/D \right)_{stg1} / \Pi_{e1} \right] \tag{18}$$

Variables *Z* and *Ze* are derived parameters for vehicle mass ratio and empty mass ratio that help in determining the viability TSTO/SSTO vehicle configuration. The $\Gamma$, $\Pi_e$ and (L/D) variables represent mass ratios for SSTO and TSTO configurations, mass fraction for empty first stage and lift-to-drag ratio also for first stage of vehicle respectively. These are also the optimization variables of large vehicle configuration.

*R. Aggregate Objective Function*

In order to avoid any conflict arising from multiple objective functions, an overall (aggregate) objective function is constructed by linear combination of multiple objective functions as shown in (12).

$$F = \left[ \sum_{i=1}^{17} \omega_i f_i \right] \Big/ \omega_3 \tag{19}$$

where $\omega$ values are weightages needed to adjust AOF value to $O(1)$.

$$\omega_1 = O(1);\ \omega_2 = O(-2);\ \omega_3 = O(2);\ \omega_4 = O(14);\ \omega_5 = O(-4);$$
$$\omega_6 = O(0);\ \omega_7 = O(-1);\ \omega_8 = O(7)\ ;\ \omega_9 = O(-3);$$

The optimization problem is classified as a nonlinear programming, constrained, parametric optimization problem of real-valued, deterministic type design variables. It has non-separable multiple objective functions for multi-objective optimization, which are reconfigured into a single aggregate objective function for implementation with other evolutionary optimization algorithms. The mathematical model is defined by solution of design vector ( $\bar{X}$ ) as follows:-

$$find\ \bar{X} = \left\{ \begin{matrix} R_N; R_L; \varepsilon; k_W; \psi_{LT}; \beta_{0d}; \beta_{1d}; \\ \beta_{2d}; \beta_{3d}; \mathrm{Re}_\theta; \phi_{23}; \\ h_{\max}; \Pi_{e1}; \Pi_{e2}; \left( L/D \right)_{stg1} \end{matrix} \right\} \tag{20}$$

$$that\ \text{minimizes}\ -f\left( \bar{X} \right) = \text{maximizes}\ g\left( \bar{X} \right)$$

Subject to inequality constraints defined at Table I TABLE Ithese values correspond to nominal operating range parameters for hypersonic compression surfaces. The aggregate objective function $f(\overline{X})$ is defined as a vector of multiple objective functions and is defined as follows:-

$$f(\overline{X}) = \left\{ f_1(\overline{X}); f_2(\overline{X}); \ldots . f_{16}(\overline{X}); f_{17}(\overline{X}) \right\} \quad (21)$$

where $f_i(\overline{X})$ for $i$ = 1 to 17 is defined by (1) to (18) while aggregate function $f(\overline{X})$ is defined by (19) and (21) from above.

## IV. Two-Step SVM Classification Approach

The process of implementing SVM in mass-model classification of TSTO surrogates cannot be complied directly without first carrying out segregation and pre-classification of training data obtained from the SHWAMIDOF program. Therefore implementation of SVM in TSTO mass-model classification is a two-step process. The first step called *segregation & pre-classification step* is followed by *SVM training & classification step*. Fig. 4 depicts the schematics of SVM implementation algorithm in TSTO classification process.

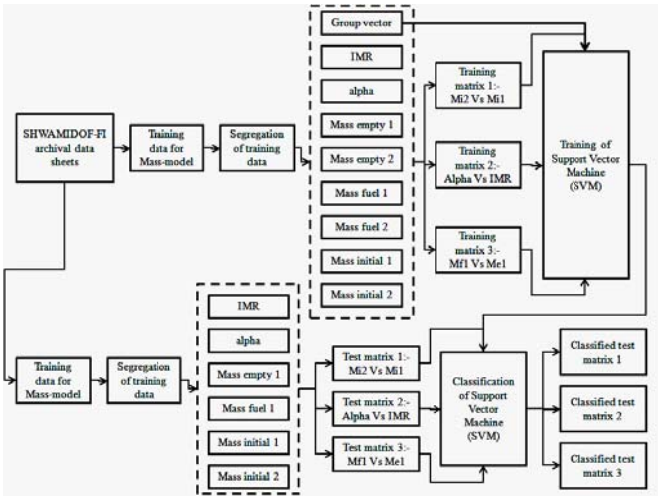


Fig. 4 The two-step SVM process for mass-model classification of TSTO vehicle

### A. Step 1

The training data obtained from previous SHWAMIDOF-FI runs does not contain information about classes in which the data can be categorized, therefore the mass-model data is first segregated i.e. text and numerical data of all variables is separated and numerical data is stored into smaller sub-matrices which contain only the desired comparative data. In this way data of unnecessary parameters can be expulsed from classification process thereby saving both computational effort and time while reducing the complexity of the problem. In this research three sub-matrices are generated as follows:-

1. *Training matrix 1* – comparison between initial (all up) masses of first stage as function of mass of the second stage.
2. *Training matrix 2* – comparison between initial mass ratio (IMR or $\Gamma_{TSTO}$) of the TSTO vehicle as function of energy split coefficient (alpha or α).
3. *Training matrix 3* – comparison between empty mass of first stage as a function of fuel mass of the same stage.

After segregation the pre-classification is achieved by using a spreadsheet solution for training data, whereby data for the three types of training matrices (as mentioned earlier) is pre-classified by using the following functions:-

1. Training Matrix 1:- $mi_1^2$ *Vs* $(mi_1/mi_2 - 5.0)^2$

A logarithmic function in higher dimensional space for pre-classification hyperplane as defined by (22) is used. The variables $m_{i1}$ and $m_{i2}$ represent initial masses of first and second stages of TSTO respectively. The value of 5.0 in the relation for variable y refers to the nominal value of mass ratios between the first and second stages obtained from the training data.

$$y = 2.2641\ln(x) - 49.571$$
$$where\ y = \left( m_{i1}/m_{i2} - 5.0 \right)^2\ and\ x = m_{i1}^{\ 2} \quad (22)$$

2. Training Matrix 2:- $(\alpha\text{-}0.6)^2$ *Vs* $\Gamma_{TSTO}$

An exponential function is used to define the pre-classification hyperplane, as shown in (23). The variable $\Gamma_{TSTO}$ and α represent initial mass ratio of TSTO and hypersonic energy partition value respectively. The value of 0.6 used in definition of variable *x* refers to the nominal value of energy split obtained for trans-atmospheric flight using HEP method.

$$y = 9.9857e^{11.249x}$$
$$where\ y = \Gamma_{TSTO}\ and\ x = (\alpha - 0.6)^2 \quad (23)$$

3. Training Matrix 3:- $mf_1^2$ *Vs* $(me_1/mf_1)^2$

The pre-classification hyperplane is defined by a 3rd order polynomial function as shown in (24). Here the variables $m_{ei}$ and $m_{f1}$ represent empty and fuel masses of first stage (booster) of TSTO vehicle.

$$y = 8*10^{-31}x^3 - 7*10^{-20}x^2 + 1*10^{-9}x - 0.0189$$
$$where\ y = \left( m_{e1}/m_{f1} \right)^2\ and\ x = m_{f1}^{\ 2} \quad (24)$$

The pre-classification segregates training data into two classes called good and bad that represent suitable/acceptable configurations and unsuitable configurations (that need to be reworked) respectively. The pre-classified data and its groups can now be read into the main SVM function to reclassify the training data into groups defined from the pre-classification process.

*B. Step 2*

In the SVM training and classification step the training matrices together with grouping vector is passed to the SVM training function for training of data based on the pattern of grouping solution for each of training matrices. The SVM training function uses an optimization method to identify support vectors $s_i$, weight $a_i$ and bias $b$ that are used to classify vectors $x$ according to (25).

$$c = \sum_i a_i k\left(s_i, x\right) + b \tag{25}$$

Here $k$ is a kernel function and SVM training function can classify data using linear, quadratic, polynomial, Gaussian radial basis, and/or multilayer perceptron kernel functions. The classification parameter $c$ will classify data of vector $x$ as member of the first group if $c \geq 0$ otherwise it is classified as a member of the second group. Once this step is complete then new i.e. test data is generated from a fresh run of SHWAMIDOF program and mass-model data from the analysis module is passed to the SVM classifier function. As with training data the test data also goes through segregation into test matrices and is then read into the SVM classifier function which also acquires classified training data from the SVM training function. The classifier function correlates test data with training data to determine the pattern and hence predicts the possible classification of test data into the *good* and *bad* configuration categories.

## V. TIPSO-SVM Expert System Results

*A. The TIPSO Results of Baseline Optimization*

In this section the full case scenario for aerothermodynamic optimization of hypersonic compression system coupled with mass-model optimization of lower-stage TSTO vehicle is addressed for the selected baseline configuration and using the chosen global TIPSO optimizer. The optimization variables constitute geometric, aerothermodynamic and mass-modeling parameters as defined in Table I. These variables also indicate to the diversity of parameters that are required to be handled for which the TIPSO algorithm is employed.

TABLE I
Lower and Upper Bound Constraints for TIPSO Optimization Problem

| Variable | | (≥) Lower bound | (≤) Upper bound |
|---|---|---|---|
| Nose radius (m) | $R_N$ | 0.0010 | 0.0030 |
| Lip radius (m) | $R_L$ | 0.0030 | 0.0045 |
| Thermal emissivity | $\varepsilon$ | 0.90 | 0.97 |
| Thermal conductivity (W/m$^2$) | $k_w$ | 100 | 110 |
| Temperature factor laminar-to-turbulent | $\psi_{LT}$ | 1.40 | 1.50 |
| Forebody oblique shock angle (deg) | $\beta_{0d}$ | 9.60 | 11.0 |
| 1st ramp oblique shock angle (deg) | $\beta_{1d}$ | 22.0 | 24.0 |
| 2nd ramp oblique shock angle (deg) | $\beta_{2d}$ | 26.0 | 28.0 |
| Cowl shock angle (deg) | $\beta_{3d}$ | 40.0 | 45.0 |
| Reynolds number of momentum boundary | $Re_\theta$ | 10000 | 15000 |
| Pressure factor across isolator | $\Phi_{23}$ | 1.40 | 1.50 |
| Max. height of generating cone (m) | $h_{max}$ | 10.0 | 12.0 |
| Empty mass fraction of stage 1 | $\Pi_{e1}$ | 0.35 | 0.42 |
| Empty mass fraction of stage 2 | $\Pi_{e2}$ | 0.19 | 0.22 |
| Lift-to-drag ratio of stage 1 | $(L/D)_{stg1}$ | 4.0 | 5.0 |

The outcome of TIPSO optimization is the optimal variables. These are compared with corresponding variables of baseline configurations at Table II to determine the percentage change brought about by optimization. The percent variations show that heuristic optimization affects all parameters of optimization some of which are increased while others are reduced in comparison with baseline parameters. An assessment based on baseline parameters vis-à-vis the optimal results can be assessed rather easily by evaluating and comparing performance, geometric and mass-modeling parameters corresponding to the baseline and optimal configurations.

TABLE II
Comparative Results of Optimization Variables for Baseline and Optimal Configurations

| Variables | | Baseline | Optimal | Variation (%) |
|---|---|---|---|---|
| Nose radius (m) | $R_N$ | 0.0025 | 0.001359 | -45.64 |
| Lip radius (m) | $R_L$ | 0.0025 | 0.003628 | +45.12 |
| Thermal emissivity | $\varepsilon$ | 0.90 | 0.9309 | +3.433 |
| Thermal conductivity (W/m$^2$) | $k_w$ | 200 | 109.07 | -45.46 |
| Temperature factor laminar-to-turbulent | $\psi_{LT}$ | 1.50 | 1.4568 | -2.88 |
| Forebody oblique shock angle (deg) | $\beta_{0d}$ | 10 | 9.6084 | -3.916 |
| 1st ramp oblique shock angle (deg) | $\beta_{1d}$ | 23.11 | 22.28 | -3.59 |
| 2nd ramp oblique shock angle (deg) | $\beta_{2d}$ | 27.57 | 26.61 | -3.48 |
| Cowl shock angle (deg) | $\beta_{3d}$ | 43.29 | 41.36 | -4.46 |
| Reynolds number of momentum boundary | $Re_\theta$ | 8000 | 14483 | +81.04 |
| Pressure factor across isolator | $\Phi_{23}$ | 1.5 | 1.4071 | -6.19 |
| Max. height of generating cone (m) | $h_{max}$ | 15 | 11.69 | -22.06 |
| Empty mass fraction of stage 1 | $\Pi_{e1}$ | 0.40 | 0.3701 | -7.48 |
| Empty mass fraction of stage 2 | $\Pi_{e2}$ | 0.21 | 0.1926 | -8.28 |
| Lift-to-drag ratio of stage 1 | $(L/D)_{stg1}$ | 4.5 | 4.7487 | +5.52 |

Table III represents the comparative parameters for both configurations. These results show that cognitive heuristic framework yields an optimized configuration with higher overall efficiency. An increase in cycle temperature and pressure is seen as useful for combustion efficiency and equivalent specific thrust. However temperature and pressure gains cause increment in entropy and flow momentum losses which are compensated by forebody blending. In the process of configuration optimization it is envisaged that the geometry of baseline configuration will be re-sized so as to proportionately reduce the dimensions of the forebody-inlet assembly while attendantly increasing inlet flow capture area and improving the lift-to-drag and net thrust behavior of the system. Results of Table III show that for minimal variations in dimensions along axial and vertical direction but substantial reduction of upto 20% in frontal area (spurred by considerable variations along lateral direction) of the system, optimization process yields an optimal configuration by utilizing a waverider of 57% smaller base dimension. The inlet size gets increased by nearly 10% while the isolator throat is widened by four folds hence providing flow relieving effect that would permit higher Mach number operations to be performed by the system. The larger air inlet results in weaker sidewall and boundary layer interaction effects and hence an improved starting performance. Optimization results show that energy split parameter (α) shifts in favor of lower stage of TSTO vehicle, an improved TSTO mass configuration is achieved with as much substantial reduction in launch weight. Under the improved configuration both Z and $Z_e$ parameters reduce below unity value hence the mass ratio of CAV stage holds good for both SSTO and TSTO configurations.

TABLE III
COMPARATIVE PARAMETERS FOR BASELINE AND TIPSO OPTIMIZED CONFIGURATION

| Parameters | Baseline config. | Optimal config. |
|---|---|---|
| Compression efficiency ($\eta_c$) | 0.8932 | 0.8944 |
| Cycle temperature ratio (Ψ) | 4.54 | 4.34 |
| Cycle pressure ratio (φ) | 121.6 | 105.84 |
| Cycle entropy change ratio (χ) | 0.3124 | 0.3016 |
| Mass flow specific thrust ($F_{sp}$) | 685 m/s | 719 m/s |
| Uninstalled thrust ($F_{uninst}$) | 27KN | 29KN |
| Specific impulse ($I_{sp}$) | 2402s | 2521s |
| Overall (aeroth.) efficiency ($\eta_o$) | 0.3634 | 0.3814 |
| Hypersonic energy partition (α) | 0.64 | 0.725 |
| Payload mass ($m_{pay}$) | 7000 | 7000 |
| Empty mass of TSTO ($m_e$) | 48391 | 30880 |
| Fuel mass TSTO ($m_f$) | 55303 | 37712 |
| Launch mass TSTO ($m_{total}$) | 110695 | 75592 |
| SSTO vs TSTO ($Z/Z_e$) | 1.15/1.08 | 0.97/0.88 |

### *B. Mass-Modeling Parameters*

Since mass-modeling forms the basis of classification work for the TSTO configuration, therefore it is imperative to exclusively compile the mass-modeling parameters for the optimized vehicle. The mass data is evaluated on the basis of hypersonic energy partition (HEP) principle [10] and calculated for various pseudo-orbit altitude above mean sea level (AMSL) up to nominal low earth orbit (LEO). Selected results are presented at Table IV below. Insofar as distribution of vehicle masses are concerned between the first and second stages a minimum initial mass ratio configuration is considered to be the most feasible. Therefore the mass-model at 6536 km altitude is selected as the optimal masses for the TSTO stages and the optimal LEO (low earth orbit) height is defined at 165km. It is the mass-model parameters at this altitude that are processed through SVM for evaluating the suitability of the evolved optimal configuration.

TABLE IV
MASS MODELING PARAMETERS OF OPTIMIZED TSTO CONFIGURATION

| Orbital radius (km) | Initial mass ratio ($\Gamma_{TSTO}$) | Energy split (α) | Empty mass | | Fuel mass stage | | Gross mass | |
|---|---|---|---|---|---|---|---|---|
| | | | Stage 1 ($m_{e1}$) | Stage 2 ($m_{e2}$) | Stage 1 ($m_{f1}$) | Stage 2 ($m_{f2}$) | Stage 2 ($m_{i2}$) | vehicle ($m_{ish}$) |
| 6486 | 12.962 | 0.509 | 33582.7 | 5332.9 | 29459.2 | 15360.4 | 27693.3 | 90735.2 |
| 6496 | 12.127 | 0.552 | 31418.8 | 4619 | 29483.5 | 12367.2 | 23986.2 | 84888.5 |
| 6506 | 11.538 | 0.596 | 29892.1 | 4054.2 | 29818.3 | 9999 | 21053.2 | 80763.6 |
| 6516 | 11.139 | 0.639 | 28859.5 | 3596.6 | 30437.2 | 8080.4 | 18677 | 77973.7 |
| 6526 | 10.899 | 0.682 | 28236.6 | 3218.8 | 31339.3 | 6496.2 | 16715 | 76290.9 |
| 6536 | 10.799 | 0.725 | 27978 | 2901.9 | 32544.8 | 5167.4 | 15069.3 | 75592.1 |
| 6546 | 10.799 | 0.725 | 28043.5 | 2901.9 | 32656.2 | 5167.4 | 15069.3 | 75769 |
| 6556 | 10.799 | 0.725 | 28109 | 2901.9 | 32767.8 | 5167.4 | 15069.3 | 75946.1 |
| 6566 | 10.799 | 0.725 | 28174.6 | 2901.9 | 32879.4 | 5167.4 | 15069.3 | 76123.3 |

### *C. SVM Based Expert System Results*

Hereinafter the optimized configuration is designated as FIC-2113MEO. The pre-classified data and its groups are read into the SVM which employs (25) to reclassify the training data into groups defined from the pre-classification process. In the training process of SVM data a *linear kernel* function is employed to map the training data of the three matrices into kernel space. The separating hyperplane for training data is found by using sequential minimal optimization (SMO) method. Results obtained for the classification of FIC-2113MEO configuration matrices are presented in Figs. 5~7 below. Results of Fig. 5 depict that test data of mass-model obtained from FIC-2113MEO is classified into the *good* category. This implies that for a certain value of initial mass of lower-stage of TSTO the mass ratio between lower and upper stages will be a minimal value hence providing for a lighter

TSTO configuration at launch. In Fig. 6 test data of mass-model obtained from FIC-2113MEO is also classified into the *good* category. This shows that the variation in energy split ratio of test data and nominal results has a minimizing tendency and that the subject energy split results in a vehicle which attendantly has minimizing tendency in initial mass ratio. This in general implies that FIC-2113MEO has an optimal divisioning of thrust required to be delivered by the first and second stages along with minimization of overall vehicle mass per kilogram of payload being carried into orbit. Results at Fig. 7 also depict that FIC-2113MEO has a *good* configuration insofar as mass-model is concerned. In the correlation of empty mass of lower-stage with of fuel mass also of the same stage, it is seen that the test configuration produces lower values of square of mass ratio ($m_{e1}/m_{f1}$) as function of change in the square of fuel mass of first stage of TSTO. This implies that for any amount of liquid hydrogen fuel added in the first stage of TSTO spaceplane the corresponding total stage-weight of optimized configuration will remain minimal.

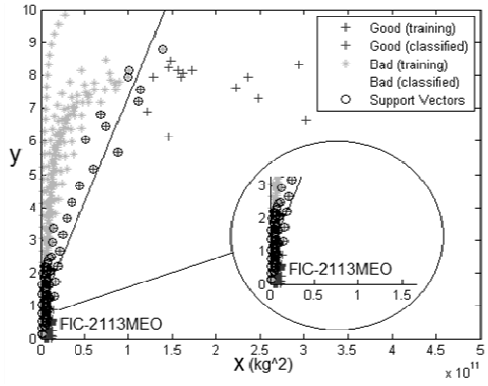


Fig. 5 Two-step SVM classification results of FIC-2113MEO

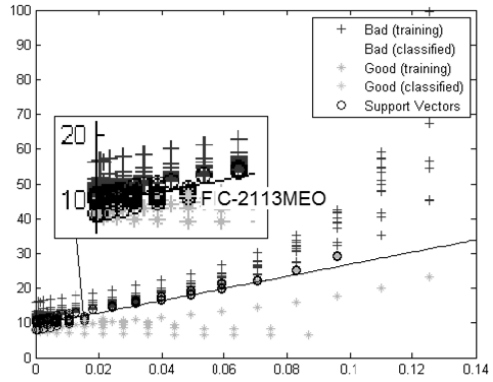


Fig. 6 Two-step SVM classification results of FIC-2113MEO

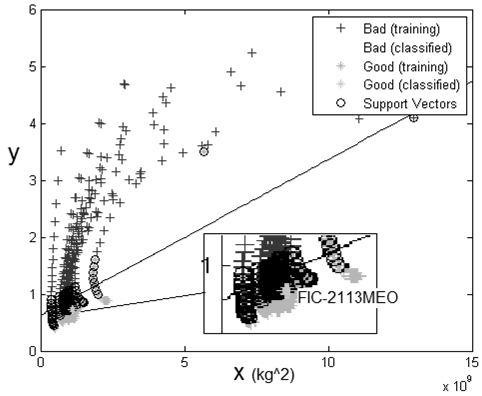


Fig. 7 Two-step SVM classification results of FIC-2113MEO

Classification results of optimized configuration FIC-2113MEO for each of the test matrices are summarized at Table V below.

TABLE V
CLASSIFICATION RESULTS OF TWO-STEP SVM METHOD FOR FIC-2113MEO

| Property | Matrices | Classification |
|---|---|---|
| Initial masses of stages | Type 1 (22) | 'good' |
| Mass ratios and energy split | Type 2 (23) | 'good' |
| Fuel and empty masses | Type 3 (24) | 'good' |

The results obtained through classification of mass-modeling data, using artificially intelligent solution based on SVM method, vindicate the efficacy of optimized solution produced by SHWAMIDOF-FI program. In that the test configuration FIC-2113MEO has the lightest possible mass-model as may be necessary to evolve a *good* configuration for a TSTO spaceplane to LEO destinations. Since the above configuration has been evaluated as suitable for TSTO application therefore vehicle sizing is undertaken. This is accomplished using HASA sizing methodology for TSTO spaceplanes and results at Table VI show that the TIPSO optimized and SVM classified configuration shows remarkable improvement in vehicle sizing characteristics. These results imply that TIPSO-SVM hybridized methodology in effect leads to substantial improvement in aerospace vehicle sizing and is attendantly able to classify the surrogates correctly thereby leading to selection of surrogates that show improved parameters only.

TABLE VI
BASELINE AND EVOLVED SIZING PARAMETERS OF TSTO BOOSTER

| Parameters | Baseline | Optimized |
|---|---|---|
| Total volume ($m^3$) | 1352.01 | 896.05 |
| Empty volume ($m^3$) | 691.05 | 436.65 |
| Fuel volume ($m^3$) | 661.0 | 459.4 |
| Total wetted area $m^2$) | 1106.13 | 939.5 |

## VI. CONCLUSION

A hybridized inverse design methodology that incorporates TIPSO optimization and SVM classification is proposed as part of an expert system to optimize and classify surrogates of TSTO vehicles. The methodology is unique in that it does not

rely on archival design data and instead a fast and frugal approach accumulates high-fidelity optimal solution data necessary for training of computational machine. A two-step SVM algorithm segregates text and numerical data from optimized solution and classifies the results of all newly generated optimization solution of TSTO surrogates. Classification results have been consistent with physical parameters of surrogates and the methodology is deemed to be of extensive utility as an expert system that relies on self-generated training data and is independent of archival information from other aerospace systems.

## REFERENCES

[1] L. Jian-xia, H. Zhong-xi, and C. Xiao-qing, "Numerical-Study-of-Hypersonic-Glide-Vehicle-Based-On Blunted-Waverider," *World Academy of Science, Engineering and Technology,* vol. 55, 2011.

[2] A. Charoenpon and E. Pankeaw, "Method-of-Finding-Aerodynamic-Characteristic-Equations-of-Missile-for-Trajectory-Simulation," *World Academy of Science, Engineering and Technology,* vol. 57, 2011.

[3] J. Cecrdle and J. Malecek, "Conceptual-Design-of-Aeroelastic-Demonstrator-for-Whirl-Flutter-Simulation," *World Academy of Science, Engineering and Technology,* vol. 68, 2012.

[4] G. Rubio, E. Valero, and S. Lanzan, "Computational-Fluid-Dynamics-Expert-System-using-Artificial-Neural-Networks," *World Academy of Science, Engineering and Technology,* vol. 63, 2012.

[5] D. Hu, A. Sarosh, and Y.-F. Dong, "An Improved Particle Swarm Optimizer for Parametric Optimization of Flexible Satellite Controller," *Applied Mathematics and Computation,* vol. 217, pp. 8512-8521, 2011.

[6] A. Sarosh, H. Di, and D. Yun-Feng, "A TIPSO Algorithm Assessment for Aerothermodynamic Optimization of Hypersonic Compression Systems," *Engineering Optimization,* vol. 45, pp. 591-608, 2013.

[7] Sarosh, D. Yun-Feng, and M. Shoaib, "An Aerothermodynamic and Mass-Model Integrated Optimization Framework for Highly-Integrated Forebody-Inlet Configurations," *Applied Mechanics and Materials,* vol. 245, pp. 277-282, 2013.

[8] Marsh, P. M. Todd, and G. Gigerenzer, "Cognitive Heuristics," *JP Leighton and RJ Sternberg (ed. s), The Nature of Reasoning, Cambridge University Press, Cambridge, MA, USA,* pp. 273-287, 2004.

[9] Sarosh, C. Shi-Ming, and D. Yun-Feng, "A Difference-Fractional FOM Decision Method for Down-Selection of Hypersonic Compression System Configurations," *Aerospace Science and Technology,* 2012.

[10] P. Ortwerth, "Scramjet Flowpath Integration," *Scramjet Propulsion, Reston, VA, American Institute of Aeronautics and Astronautics, Inc., 2000,* pp. 1105-1293, 2000.